Article

EGFR Targeted Polymeric Mixed Micelles carrying Gemcitabine for treating Pancreatic Cancer

Goutam Mondal, Virender Kumar, surendra K Shukla, Pankaj K Singh, and Ram I. Mahato

Biomacromolecules, **Just Accepted Manuscript** • DOI: 10.1021/acs.biomac.5b01419 • Publication Date (Web): 01 Dec 2015

ACS Publications

Biomacromolecules is published by the American Chemical Society. 1155 Sixteenth Street N.W., Washington, DC 20036

EGFR Targeted Polymeric Mixed Micelles carrying Gemcitabine for treating Pancreatic Cancer

Goutam Mondal[1], Virender Kumar[1], Surendra K. Shukla[2], Pankaj K. Singh[2] and Ram I. Mahato [1]*

[1]Department of Pharmaceutical Sciences, University of Nebraska Medical Center, Omaha, NE 68198

[2]Department of Biochemistry and Molecular Biology, University of Nebraska Medical Center, Omaha, Nebraska, USA

*Corresponding Author

Ram I. Mahato, Ph.D.

Department of Pharmaceutical Sciences

University of Nebraska Medical Center

986025 Nebraska Medical Center

Omaha, NE 68198

Tel: (402)559-5422, Fax: (402)559-9543

E-mail: ram.mahato@unmc.edu

ABSTRACT

The objective of this study was to design GE11 peptide (YHWYGYTPQNVI) linked micelles of poly(ethyleneglycol)-block-poly(2-methyl-2-carboxyl-propylenecarbonate-graft-gemcitabine-graft-dodecanol (PEG-b-PCC-g-GEM-g-DC) for enhanced stability and target specificity of gemcitabine (GEM) to EGFR positive pancreatic cancer cells. GE11-PEG-PCD/mPEG-b-PCC-g-GEM-g-DC mixed micelles showed EGFR dependent enhanced cellular uptake, and cytotoxicity as compared to scrambled peptide HW12-PEG-PCD/mPEG-b-PCC-g-GEM-g-DC mixed micelles and un-modified mPEG-b-PCC-g-GEM-g-DC micelles. Importantly, GE11-linked mixed micelles preferentially accumulated in orthotopic pancreatic tumor and tumor vasculature at 24 h post systemic administration. GE11-linked mixed micelles inhibited orthotopic pancreatic tumor growth compared to HW12-linked mixed micelles, un-modified mPEG-b-PCC-g-GEM-g-DC micelles and free GEM formulations. Tumor growth inhibition was mediated by apoptosis of tumor cells and endothelial cells as determined by immunohistochemical staining. In summary, GE11-linked mixed micelles is a promising approach to treat EGFR overexpressing cancers.

Keywords: pancreatic cancer, epidermal growth factor receptor, EGFR, polymeric mixed micelles, gemcitabine.

1. INTRODUCTION

Pancreatic ductal adenocarcinoma (PDAC) is the fourth leading cause of cancer related death in the United States due to poor prognosis and high metastasis.[1-3] Conventional chemotherapy often fails to treat pancreatic cancer and often causes non-specific toxicity to healthy tissues. Gemcitabine (GEM) a nucleoside analogue is the first line chemotherapy to treat PDAC with a mere 6.8 month survival rate, and up to 11.1 months as combination therapy.[4-6] GEM exhibits its anticancer activity through blocking DNA replication and inducing S-phase cell cycle arrest. However, due to its rapid metabolism into inactive form 2'-deoxy-2', 2'-difluorodeoxyuridine (dFdU) and non-specific toxicity reduces its therapeutic potential.[7, 8]

Various drug delivery systems like liposomes, nanoparticles and micelles fail to improve GEM plasma stability due to poor drug loading and premature release.[9-13] Chemical conjugation of GEM to lipid or polymeric carriers has been shown to improve its loading but has lower aqueous solubility.[14, 15] To overcome these challenges, squalenoyl derivatives of GEM were developed, however their efficacy was limited due to the rapid uptake by the reticuloendothelial system (RES).[16] Since the incorporation of polyethylene glycol (PEG) onto polymeric systems provides stealth properties and prolonged circulation, we recently synthesized methoxy poly(ethyleneglycol)-block-poly(2-methyl-2-carboxyl-propylenecarbonate-graft-gemcitabine-graft-dodecanol (mPEG-b-PCC-g-GEM-g-DC), where PEG corona ensures stealth properties and the presence of carboxyl groups in polymeric backbone enables higher GEM loading. This polymeric system self-assembled into micelles and inhibited subcutaneous xenograft tumor after intravenous administration.[17] However, passive targeting is effective only in

highly vascularized and rapidly growing tumors, but it is not effective in poorly vascularized and metastatic tumors.[18] Since tumor progression, invasion and metastasis critically depend on endothelial cells derived angiogenesis, selective delivery of anticancer agents to the tumor endothelial cells is an attractive approach.[19, 20] To date, a very few targeted nanoparticles are reported for drug delivery to the tumor and its vasculature for pancreatic cancer treatment.[21]

Epidermal growth factor receptor (EGFR) is overexpressed in the tumor derived neovasculature of pancreatic tumor.[22] Full length EGFR natural ligand, such as EGF and monoclonal antibody cetuximab conjugated nanoparticles have been shown to enhance the receptor-mediated endocytosis of GEM by pancreatic tumor cells.[23] However, high mitogenic and pro-angiogenic capability of full length EGFR ligands retard their clinical translation. Alternatively, GE11 peptide (YHWYGYTPQNVI) ligand has been shown its specific binding to EGFR with low mitogenic activity.[24] Moreover, GE11 peptide decorated delivery systems efficiently deliver drugs/genes to EGFR overexpressing cancer cells.[25-27]

In this study, we conjugated GE11 peptide to the surface of malemido-poly (ethylene glycol)-block-poly (2-methyl-2-carboxyl-propylene carbonate-graft-dodecanol (GE11-PEG-PCD) and synthesized methoxy-poly (ethylene glycol)-block-poly (2-methyl-2-carboxylpropylene carbonate-graft-gemcitabine-graft-dodecanol (mPEG-b-PCC-g-GEM-g-DC) to prepare mixed micelles for enhanced GEM delivery to EGFR expressing pancreatic cancer cells. We showed that GE11 linked mixed micelles exhibited a better therapeutic effect than non-targeted mixed micelles in vitro and in MIA PaCa-2 cells derived orthotopic pancreatic tumor bearing mice.

2. EXPERIMENTAL SECTION

2.1. Materials

N-terminal cysteine containing GE11 peptide was custom synthesized by Shanghai Hanhong Chemical Co. Ltd. (Shanghai, China). Its purity and structure were confirmed by HPLC (purity 98.36 %) and ^{1}H-NMR. N-terminal cysteine containing CHYPYAHPTHPSW (designated as HW12) peptide was custom synthesized by Biomatik USA, LLC (Delaware, USA). Its purity and structure were confirmed by HPLC (purity 97.58 %) and ^{1}H-NMR, respectively. Malemide PEG hydroxyl (MW 5000) was purchased from JenKem Technology (Beijing, China). Gemcitabine hydrochloride was purchased from AK Scientific (Union city, CA). Dodecanol (DC), triethylamine (TEA), 1-ethyl-3-(3-dimethylaminopropyl) carbodiimide (EDC), hydroxybenzotriazole (HOBT), 1,8-diazabicyclo[5.4.0]undec-7-ene (DBU), benzyl bromide, 2,2-bis(hydroxymethyl) propionic acid, methoxy poly(ethylene glycol) (mPEG, Mn = 5000, PDI = 1.03), puromycin dihydrochloride were purchased from Sigma Aldrich (St. Louis, MO). Matrigel® matrix basement membrane was procured from Corning (Chicago, IL). Fluorescein cadaverine (FC) dihydrobromide salt was purchased from Life Technology (Chicago, IL). Tris-(2-carboxyethyl) phosphine hydrochloride (TCEP) was purchased from Biosynth Chemistry & Biology (Itasca, IL). Polybrene and VE-cadherin (H-72) were purchased from Santa Cruz Biotechnology (Dallas, TX). Rat anti-mouse CD31 was purchased from BD Biosciences (San Diego, CA). Lentiviral particle LP-hLUC-Lv201-0200 was purchased from GeneCopoeia (Rockville, MD). Dead End™ Fluorometric TUNEL System was purchased from Promega Corporation (Madison, WI). Mouse monoclonal antibodies to EGFR (Phycoerythrin) and mouse IgG1 monoclonal

antibodies (Phycoerythrin)-Isotype control were purchased from Abchem (Cambridge, MA). Alexa Fluor 594 F(ab')$_2$ fragment of goat anti-rabbit IgG (H+L) was purchased from Invitrogen (Grand Island, NY). All other chemicals were of analytical grade and purchased from Sigma Aldrich (St. Louis, MO).

2.2. Synthesis of polymers

2.2.1. Synthesis of maleimido poly(ethylene glycol)-block-poly(2-methyl-2-dodecanoxycarbonylpropylene carbonate) (MAL-PEG-PCD)

2-Methyl-2-benzyloxycarbonylpropylene carbonate (MBC) was synthesized and converted to 2-methyl-2-carboxylpropylene carbonate (MCC) by hydrogenation reaction as reported by Li et al.[28] DC was conjugated to the carboxyl group of MCC by carbodiimide chemistry. Briefly, MTC-OH (480 mg) was dissolved in 20 mL of DMF followed by the addition of HOBT (506 mg), EDC (720 mg) and 490 µL of TEA. After 1h, DC (465 mg) was added to the reaction mixture and allowed the reaction for 18 h under N_2 atmosphere at RT. Then, ethyl acetate (20 mL) was added to the reaction mixture and the organic layer was washed with distilled water, and organic solvent dried over Na_2SO_4. The organic solvent was evaporated under reduced pressure to yield 2-methyl-2-dodecanoxycarbonylpropylene carbonate (MDC), which was purified by column chromatography.

2.2.2. Synthesis of MAL-PEG-PCD from copolymerization of MAL-PEG-OH with MDC.

MAL-PEG-OH and MDC were dissolved in 15 mL anhydrous CH_2Cl_2 and stirred under N_2 atmosphere at the room temperature (RT). Then, DBU (40 µL) was dissolved in 1 mL anhydrous CH_2Cl_2 and added to the mixture and left the reaction under stirring

for 3 h. Benzoic acid was added to the reaction mixture at the end of the reaction to neutralize excess DBU and solvent was removed under reduced pressure. Then, the crude product was dissolved with the minimum amount of $CHCl_3$ and two times precipitated with cold isopropyl alcohol, followed by diethyl ether. The precipitate was dried under high vacuum at RT to get purified MAL-PEG-PCD lipopolymer.

2.2.3. Conjugation of GE11 and HW12 peptide to MAL-PEG-PCD

MAL-PEG-PCD (20 mg) was dissolved in a mixture of DMSO: distilled water (1:1 v/v, 4ml) and stirred under N_2 at RT. GE11 peptide (6.57 mg) and tris-(2-carboxyethyl) phosphine hydrochloride (TECP, 100 mM, 100 µL) were dissolved in 1 mL DMSO and added to the reaction. Then, the reaction mixture was left for 24h at RT under N_2 atmosphere with gentle stirring. Finally, the reaction mixture was dialyzed against phosphate buffer saline using 3000 MWCO dialysis tubing to remove unreacted GE11 peptide and after dialysis, lyophilization was performed to get pure GE11-PEG-PCD. The chemical conjugation of GE11 peptide in MAL-PEG-PCD lipopolymer was finally confirmed by ^{1}H-NMR analysis. We synthesized HW12-PEG-PCD polymer using the same synthetic route as the synthesis of GE11-PEG-PCD and finally this polymer was confirmed by ^{1}H-NMR analysis.

2.2.4. Synthesis of mPEG-b-PCC-graft-fluorescein cadaverine-graft-dodecanol (mPEG-b-PCC-g-FC-g-DC)

mPEG-PCC was synthesized using our previously reported method.[17] For FC and DC conjugation, mPEG-PCC (100 mg), HOBT (61 mg) and EDC (77 mg) were dissolved in 6 mL DMF and allowed for stirring for 2 h at RT under N_2 atmosphere. FC (13 mg) and DC (56 mg) were added to the reaction mixture and followed by the

addition of 120 µL DIPEA. The reaction was allowed to continue for 48 h at RT under N_2 atmosphere. The crude product was precipitated twice with an excess of cold isopropyl alcohol and then dissolved in chloroform and precipitated in cold diethyl ether. Finally, the precipitate was dissolved in acetone and dialyzed against water using 2,000 MWCO dialysis tubing and after dialysis and lyophilized to yield mPEG-b-PCC-g-FC-g-DC.

2.2.5. Synthesis of GEM and DC conjugated mPEG-PCC-g-GEM-g-DC copolymer

mPEG-PCC (300 mg), HOBT (223 mg) and EDC (317 mg) were dissolved in 12 mL DMF and stirred for 2 h, and then GEM and DC were added to the reaction mixture, followed by addition of 360 µL N,N-diisopropylethylamine (DIPEA). The reaction was left for 48 h at RT under N_2 atmosphere. The crude product was precipitated twice with excess of cold isopropyl alcohol, dissolved in chloroform and precipitated again in the cold diethyl ether. Finally, the precipitate was dissolved in acetone and dialyzed against water using 2000 MWCO dialysis tubing and lyophilized to yield mPEG-b-PCC-g-GEM-g-DC.

2.3. Quantification of GEM payload in mPEG-b-PCC-g-GEM-g-DC copolymer

The amount of GEM conjugated to the copolymer was determined by alkaline hydrolysis method as described previously.[17] Briefly 10 mg of copolymer micelles were subjected to alkaline hydrolysis in NaOH (1 N) at 40 °C for 1 h and the samples were subjected to HPLC-UV analysis used the HPLC system equipped with photodiode array detector 996 (Waters Corporation) and data acquisition and processing were performed with Empower Pro software. A 20 µL volume of the standard and sample was injected into Inertsil ODS 3 column (4.5 × 250 mm). Analytes were eluted isocratically at the flow

rate of 1 mL/min with a mobile phase of sodium acetate buffer (20mM, pH 5.5): methanol (93: 07 v/v) and the column temperature was 40 °C.

2.4. Preparation of GE11- or HW12-linked mixed micelles

GE11-PEG-PCD/mPEG-b-PCC-g-GEM-g-DC and HW12-PEG-PCD/mPEG-b-PCC-g-GEM-g-DC mixed micelles were prepared by thin film hydration as reported with slight modification.[29, 30] Briefly, GE11-PEG-PCD (10-30% weight ratio) and mPEG-b-PCC-g-GEM-g-DC (70-90% weight ratio) were dissolved in 1 ml $CHCl_3$ in a glass vial. The solvent was evaporated under reduced pressure to form thin film and dried film was kept under vacuum overnight to remove residual $CHCl_3$. 1 mL PBS (pH 7.4) was added to the vacuum dried film and vortexed for 5 min at RT. Then resulting solution was centrifuged at 5000 g for 5 min and filtrated through 0.22 μ filter membrane to obtain the micelles. FC labeled GE11-linked mixed micelles were prepared by keeping FC concentration constant (100 μM) and mixing GE11-PEG-PCD (10-30% weight ratio) with mPEG-PCD/mPEG-b-PCC-g-FC-g-DC (70- 90 w/w). Similarly, HW12-linked mixed micelles were prepared by mixing HW12-PEG-PCD and mPEG-PCD/mPEG-b-PCC-g-FC-g-DC (70/30 w/w).

2.5. Particle size measurement

Particle size distribution and surface zeta (ζ) potential of GE11-PEG-PCD/mPEG-b-PCC-g-GEM-g-DC and HW12-PEG-PCD/mPEG-b-PCC-g-GEM-g-DC mixed micelles (10 mg/mL) were determined by photon correlation spectroscopy at a scattering angle of 173° (Malvern Zetasizer).

2.6. Stable transfection of MIA PaCa-2 cells with lentiviral particles

MIA PaCa-2 cells were kindly gifted by Dr. Rakesh Singh (UNMC, Omaha, NE) and maintained in Dulbecco's Modified Eagle Medium (DMEM) containing 10% fetal bovine serum (FBS) and 1% antibiotic in an incubator at 37 °C/5% CO_2. MIA PaCa-2 cells were stably transfected with lentiviral vector encoding luciferase and green fluorescent protein (GFP) (hLUC-Lv201-0200) using polybrene according to the manufacturer's instructions. Briefly, $2x10^5$ MIA PaCa-2 cells were seeded in each well in a 6-well plate for 24 h. For each well, 2 µL of lentiviral particles was mixed with 1 µL of polybrene (10 mg/mL) and the final volume was made to 2 mL using DMEM. The transfection mixture was then incubated for 15 min at RT with occasional agitating and MIA PaCa-2 cells were washed with PBS and were incubated with the transfection mixture overnight. The medium was replaced with 2 mL fresh DMEM for an additional 48 h. The cells were trypsinized and cultured in T-75 flasks for 15 days in 10 mL DMEM containing 2 µg/mL puromycin. Every alternative day during these 15 days, the medium was removed with a fresh DMEM containing 2 µg/mL puromycin. MIA PaCa-2 cells were then grown for another four days with fresh DMEM containing a lower concentration of puromycin (1 µg/mL). Luciferase and GFP expression from stably transfected cells were confirmed by in vivo IVIS and epifluorescence microscope respectively. Finally, cells were sorted to obtain luciferase and GFP reporter gene expressing cell population using fluorescence-activated cell sorting (FACS). In vitro and in vivo experiments were performed with stable luciferase and GFP transfected cells culturing in DMEM without puromycin.

2.7. Cellular uptake studies

Cellular uptake study was carried out in MIA PaCa-2 cells using FC labeled mixed micelles. Briefly, 2×10^5 cells were seeded per well in six-well plates for 24 h. GE11-PEG-PCD/mPEG-b-PCC-g-FC-g-DC, HW12-PEG-PCD/mPEG-b-PCC-g-FC-g-DC mixed micelles and mPEG-b-PCC-g-FC-g-DC unmodified micelles were added to each well. After 12 h cells were washed with PBS and observed under an epifluorescence microscope. Further, for quantitative estimation of FC dye in cellular uptake study, cells were washed with PBS, trypsinized, again washed with cold PBS and centrifuged. Then, cells pellet was re-suspended with PBS containing 4% paraformaldehyde and kept for 10 min at RT. Cells were centrifuged, wash with PBS, re-suspended with 1 mL PBS and analyzed by a flow cytometer (BD LSRFortessa™ X-20). For competition studies, excess of free GE11 peptide was diluted with medium and added to cells 2 h prior to the addition of GE11-PEG-PCD/mPEG-b-PCC-g-FC-g-DC mixed micelles. After 12 h, the medium was discarded and cells were washed with PBS (pH 7.4) and observed under an epifluorescence microscope (Zeiss, Germany).

2.8. Cytotoxicity study

Cytotoxicity of GE11-PEG-PCD/mPEG-b-PCC-g-GEM-g-DC, HW12-PEG-PCD/mPEG-b-PCC-g-GEM-g-DC mixed micelles, mPEG-b-PCC-g-GEM-g-DC unmodified micelles and free GEM were evaluated by 3-(4,5-dimethylthiazol-2-yl)-2,5-diphenyltetrazolium bromide (MTT) assay. MIA PaCa-2 cells were seeded at a density of ~5000 cells per well in 96-well plates for 18 h and were treated with GE11-PEG-PCD/mPEG-b-PCC-g-GEM-g-DC, HW12-PEG-PCD/mPEG-b-PCC-g-GEM-g-DC mixed micelles, mPEG-b-PCC-g-GEM-g-DC unmodified micelles and free GEM having 60-500 nM concentration of GEM. The final volume in each well was adjusted to 200 µL using

complete media and left for 72 h, 10 µL of MTT solution (5mg/ mL in PBS) were added to each well and incubated for 4 h. The formazan crystals were solubilized with 200 µL of DMSO and measured the absorbance in each well with a microplate reader at 560 nm wavelength and background correction was done by subtracting absorbance at 655 nm. Results were calculated as percent cell viability = [A560 (treated cells)-background/A560 (untreated cells)-background] x 100.

2.9. In vivo distribution and targeting study

All animal experiments were performed in accordance with the NIH animal use guidelines and protocol approved by the Institutional Animal Care and Use Committee (IACUC) at the University of Nebraska Medical Center, Omaha, NE. Orthotopic pancreatic cancer mouse model was generated by implantation of MIA PaCa-2 cells using PBS: matrigel (1:1 v/v) into pancreas of 6-8 weeks old athymic nude mice (n=3). GE11-PEG-PCD/mPEG-b-PCC-g-FC-g-DC, HW12-PEG-PCD/mPEG-b-PCC-g-FC-g-DC mixed micelles and mPEG-b-PCC-g-FC-g-DC unmodified micelles were injected to mice via the tail vein. Mice were sacrificed 24 h post injection of mixed micellar formulations, tumor were harvested. 5 µM tumor cryosections were made using cryostat instrument (Leica), fixed with 10% formaldehyde in PBS and fixed tumor sections were washed with PBS and visualized under a fluorescent microscope. For tumor vasculature targeting study, same tissue sections were again fixed in 4% paraformaldehyde in PBS and stained for rabbit polyclonal anti-VE-cadherin antibody (endothelial cells, red) (1:50 in 0.5% bovine serum albumin in PBS). Then, sections were counterstained with Alexa Fluor 594 F(ab')2 fragment of goat anti-rabbit IgG (H+L) secondary antibody (10 µg/mL

in PBS). Finally, sections were mounted with SlowFade Gold antifade reagent with DAPI and snaps were taken under a inverted fluorescence microscope.

2.10. Efficacy of mixed micelle formulations in orthotopic pancreatic tumor bearing mice

After 12 days of post implantation of luciferase and GFP stably expressing $3x10^6$ MIA PaCa-2 into athymic nude mice, 100 mg/kg of D-luciferin was administered into each animal via intraperitoneal injection and bioluminescent was measured using the IVIS Imaging System (Caliper Life Sciences). These tumor bearing mice were then randomly sorted into five groups (n = 5): 1) vehicle control i.e. normal saline, 2) GE-linked mixed micelles, 3) HW12-linked mixed micelles, 4) mPEG-b-PCC-g-GEM-g-DC un modified micelles, and 5) free GEM at an equivalent dose of 40 mg/kg GEM. Treatment was started at days 12 via intravenous administration once a week for three weeks. Bioluminescent was measured at day 12, 16, 20, 24, 26 and 30. Mouse body weight was measured at day 12, 15, 18, 21, 24, 27, and 30. After final bioluminescent measurement, mice were sacrificed and tumors were excised. Then excised tumors were frozen in a cryostat at -30 °C for 2 h, cryosections were fixed with 10% formaldehyde in PBS. Fixed tumor sections were washed with PBS and immunostained for cell proliferation marker (Ki-67), apoptosis (cleaved caspase 3) and H&E. To detect tumor cell as well as tumor vasculature apoptosis induced by GEM treatment, orthotopic MIA PaCa-2 bearing mice (n = 3) were intravenously administered with GE11-linked mixed micelles, HW12-linked mixed micelles, mPEG-b-PCC-g-GEM-g-DC unmodified micelles and free GEM once a week for three weeks post tumor inoculation. Mice were sacrificed 72 h post last injection, tumors excised. Tumors were cryosectioned and fixed

cryosections were immunostained with TUNEL assay kit according to the manufacturer's instructions and counterstained with DAPI and imaged under fluorescence microscope. To measure the tumor endothelial microvessels density, tumor sections were immunostained with CD31 primary antibody.

2.11. Statistical analysis

Data are represented as means ± SEM. The statistical comparisons of the experiments were performed by two-tailed Student's test. $P < 0.05$ was considered statistically significant.

3. RESULTS AND DISCUSSION

Bioconjugation to a polymeric carrier is an attractive strategy to enhance the in vivo stability and delivery of GEM to the tumor. Several PEGylated conjugates, lipid conjugates and squalenoyl derivatives of GEM have been demonstrated to enhance its bioavailability.[14-16] However, the clinical translation of these delivery systems is limited by poor solubility, uptake by RES, and lower GEM payload. We synthesized mPEG-PCC copolymer having several carboxyl pendant groups for conjugating GEM.[17] This co-polymer could self-assemble into micelles and significantly inhibited subcutaneous MIA PaCa-2 cells implanted xenograft tumor after systemic administration. In the present study, we used GE11 peptide as a targeting ligand that efficiently binds to EGFR and has low mitogenic activity.[24] We synthesized GE11-PEG-PCD using GE11 peptide, Mal-PEG-PCD, and TCEP (**Fig. 1A**). To confirm GE11 and not HYPYAHPTHPSW (designated as HW12) is an EGFR ligand, HW12-PEG-PCD was synthesized using the same synthetic route as mentioned for synthesizing GE11-PEG-PCD (**Fig. 1B**). We also synthesized mPEG-b-PCC-g-GEM-g-DC and mPEG-b-PCC-g-

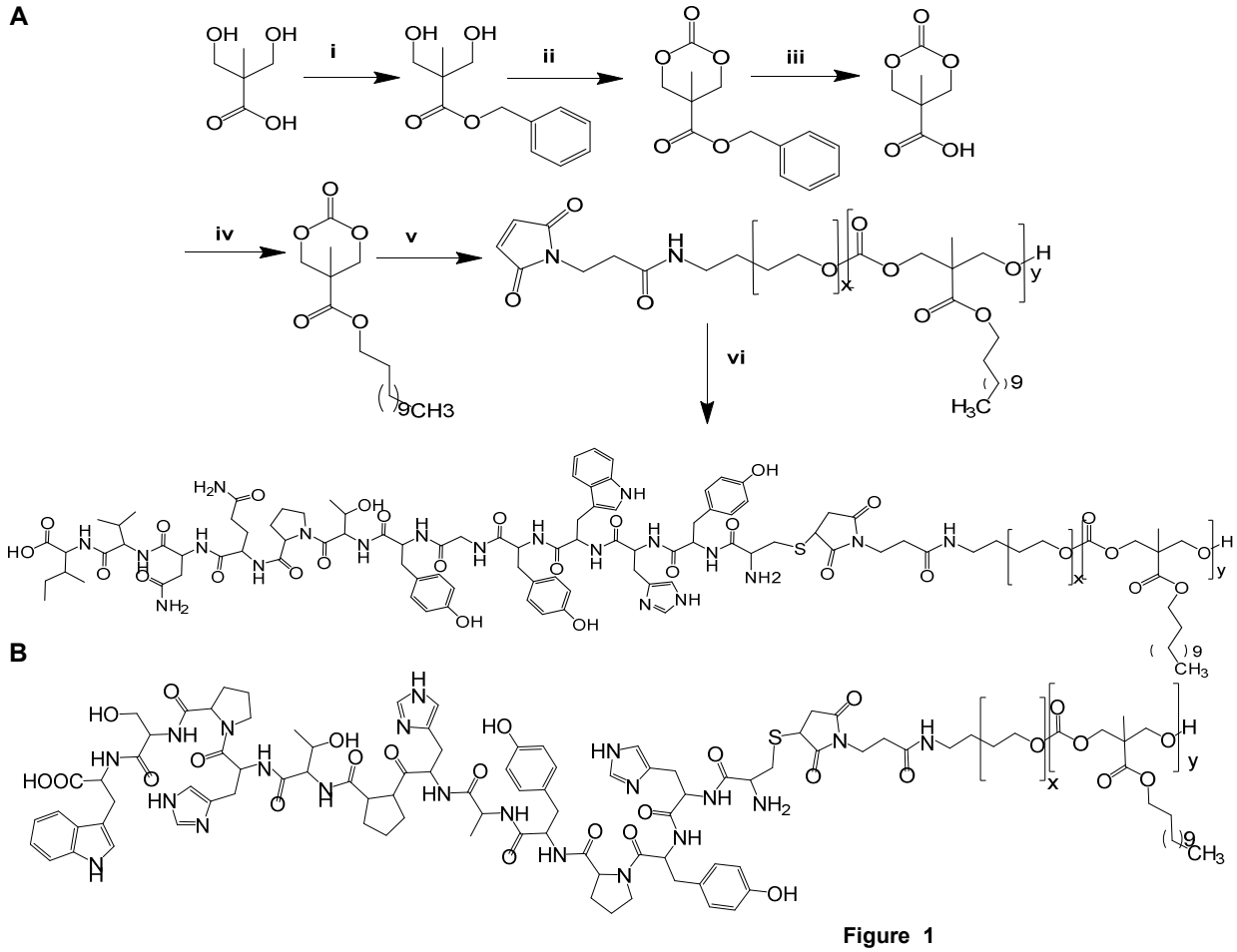

Figure 1

FC-g-DC copolymers (**Fig. 2 A&B**). It is important to note that the two components of this copolymer are biocompatible PEG block and a biodegradable polycarbonate (PCC) block. Polycarbonates are biodegradable and have low toxicity, as their degradation products are carbon dioxide and alcohol, which are less acidic, have less effect on microenvironment pH and thus will not result in local inflammation.[31]

3.1. Synthesis and characterization of GE11-PEG-PCD, HW12-PEG-PCD, mPEG-b-PCC-g-GEM-g-DC and mPEG-b-PCC-g-FC-g-DC copolymers

MBC monomer was characterized by ^{1}H NMR (500 MHz, DMSO-d_6), which showed peaks corresponding to phenyl proton at δ7.5, methylene protons present in the

carbonate ring at δ4.2 and δ4.7. Methyl and benzyl protons were present at δ1.3 and δ5.2, respectively (data not shown). MCC was obtained by hydrogenation of MBC and characterized by ^{1}H NMR (500 MHz, chloroform-*d*) δ13.35 (s, 1H), 4.57 (d, 2H), 4.32 (d, 2H) and 1.18 (s, 3H) (data not shown).

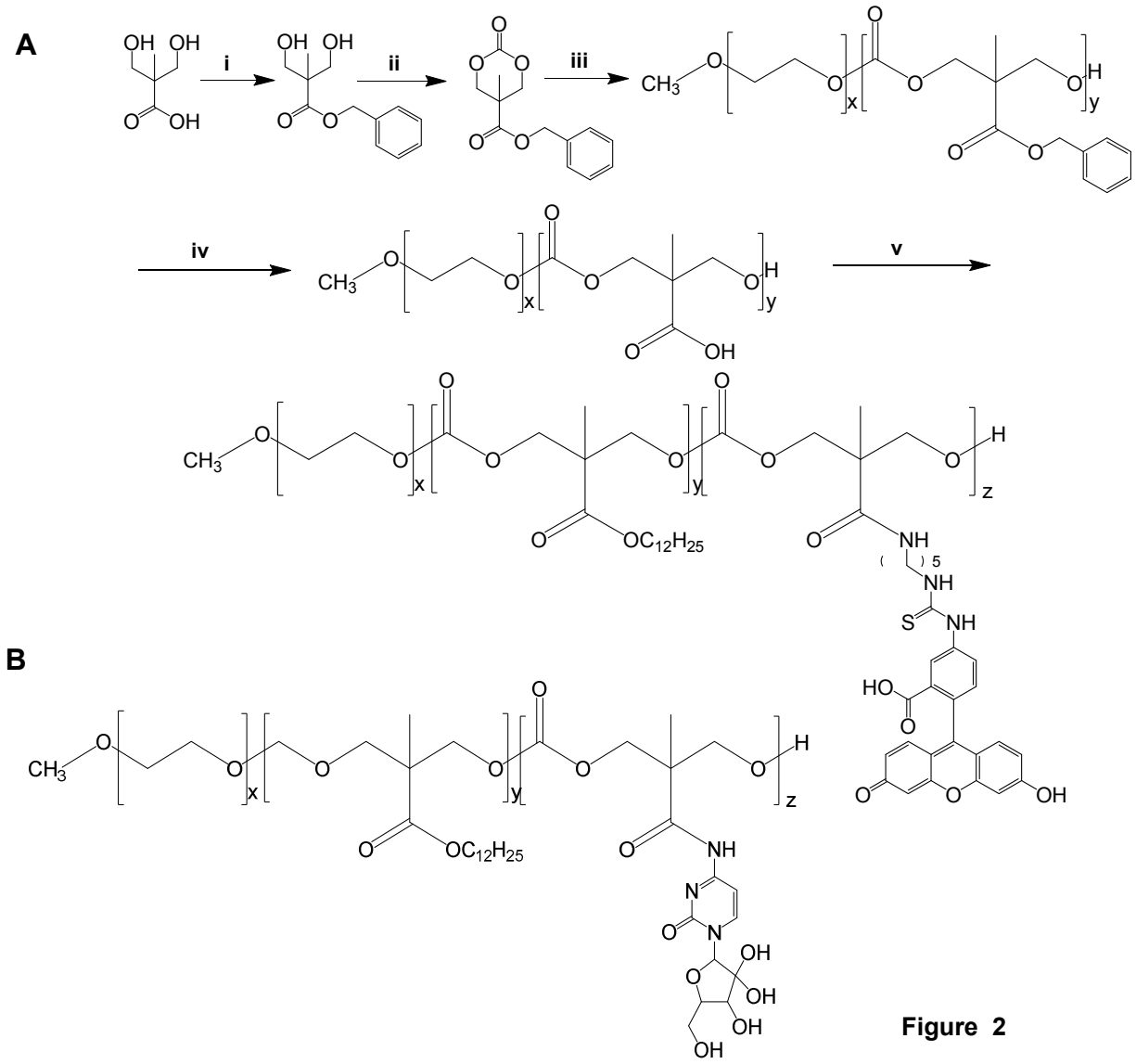

Figure 2

DC was conjugated to the carboxyl group of MCC by EDC/HOBT coupling and final product was purified by column chromatography and characterized by ^{1}H NMR (500 MHz, chloroform-*d*), with the following characteristic peaks: δ4.50 (d, 2H), 4.2 (d, 4H), 1.65 (m, 2H), 1.4-1.2 (m, 21H) and 0.85 (t, 3H) (data not shown). Ring opening

polymerization of MDC and Mal-PEG in the presence of 1,8-diazabicycloundec-7-ene (DBU) catalyst at RT for 3 h under N_2 atmosphere yielded MAL-PEG-PDC copolymer. ^{1}H NMR (500 MHz, DMSO-d_6) spectra of Mal-PEG-PDC showed peaks corresponding to PEG (−C$\underline{H}_2$−C$\underline{H}_2$−O) at δ3.5, PCC (−CO-O-C$\underline{H}_2$- & CH_3-C(CO)-C$\underline{H}_2$) at δ4.2 (m, 4H), C$\underline{H}_3$-$(CH_2)_9$- at δ0.9 (t, 3H), CH_3-(C$\underline{H}_2$)$_9$- at δ1.2-1.45 (bs, 18H), CH_3-$(CH_2)_9$-C$\underline{H}_2$ & -NH-CH_2-C$\underline{H}_2$ at δ1.5-1.8 (m, 4H), CH_3-$(CH_2)_9$-CH_2-C$\underline{H}_2$- at δ4.02 (m, 2H), -NH-C$\underline{H}_2$-CH_2 & -NH-CO-C$\underline{H}_2$-CH_2 at δ2.5-3.2 (m, 4H), -NH-CO-CH_2-C$\underline{H}_2$ at δ4.6 (m, 2H), -N$\underline{H}$-CO-CH_2-CH_2 at δ8.4 (m, 1H), -CO-C$\underline{H}$=C$\underline{H}$-CO- at δ7.2-7.5 (t, 2H) (**Fig. S1**). GE11 peptide was conjugated to MAL-PEG-PDC via the addition reaction. GE11-PEG-PCD copolymer was lyophilized and characterized using ^{1}H NMR (500 MHz, DMSO-d_6), which showed peaks corresponding to PEG (−C$\underline{H}_2$−C$\underline{H}_2$−O) at δ3.5, PCC (−CO-O-C$\underline{H}_2$- & CH_3-C(CO)-C$\underline{H}_2$) at δ4.2 (m, 4H), C$\underline{H}_3$-$(CH_2)_9$- at δ0.9 (t, 3H), CH_3-(C$\underline{H}_2$)$_9$- at δ1.2-1.45 (bs, 18H), Ile C^{β}-$\underline{H}$ at δ 2.6 (m, 1H), C^{α}-$\underline{H}$ of (Cys,Tyr, His, Trp, Thr, Pro, Gln, Asn, Val & Ile) amino acids at δ4.2-4.9 (m, 12H), Gly –C$\underline{H}_2$-NH at δ 4.4 (m, 2H), Ile C^{γ}-$\underline{H}_2$ at δ 1.5 (m, 2H), Ile C^{δ}-$\underline{H}_3$ at δ 0.9 (t, 3H), Ile C^{β}-H-C$\underline{H}_3$ at δ 1.1 (m, 3H), Val C^{β}-$\underline{H}$ at δ 2.5 (m, 1H), Val C^{β}H-C$\underline{H}_3$ and Val C^{γ}-$\underline{H}_3$ at δ 0.9 (t, 6H), Asn C^{β}-$\underline{H}_2$ at δ 2.5-2.9 (m, 2H), Gln $C^{\beta}\underline{H}_2$ and Gln C^{γ}-$\underline{H}_2$ at δ 2.1-2.3 (m, 4H), Pro C^{β}-$\underline{H}_2$ at δ 2.0-2.2 (m, 2H), Pro C^{γ}-$\underline{H}_2$ at δ 1.9-2.1 (m, 2H), Pro C^{δ}-$\underline{H}_2$ at δ 3.3-3.5 (m, 2H), Thr –CH-C$\underline{H}$(CH_3)-OH at δ 4.6 (m, 1H), Thr –CH-CH(C$\underline{H}_3$)-OH at δ 1.2 (m, 3H), Tyr C^{β}-$\underline{H}_2$ at δ 3.2-3.45 (m, 2H), Tyr–CH_2-$C_6\underline{H}_4$-OH at δ 6.5-6.9 (m, 4H), Trp C^{β}-$\underline{H}_2$ at δ 3.0-3.4 (m, 2H), Trp –CH_2-$C_8\underline{H}_5$NH at δ 7.1-8.3 (m, 5H), His C^{β}-$\underline{H}_2$ at δ 2.9-3.15 (m, 2H), His –CH_2-$C_3\underline{H}_2N_2H$ at δ 8.2-8.7 (m, 2H), Cys C^{β}-$\underline{H}_2$ at δ 2.9-3.2 (m, 2H) (**Fig. S2**). The peaks at 6.5–9.3 ppm confirmed the successful conjugation of GE11 peptide to the copolymer.[25] Similarly,

HW12-PEG-PCD was synthesized and characterized using ^{1}H NMR (500 MHz, DMSO-d_6), which showed peaks corresponding to PEG (−C$\underline{H}_2$−C$\underline{H}_2$−O) at δ3.5, PCC (−CO-O-C$\underline{H}_2$- & CH_3-C(CO)-C$\underline{H}_2$) at δ4.2 (m, 4H), C$\underline{H}_3$-(CH_2)9- at δ0.9 (t, 3H), CH_3-(C$\underline{H}_2$)9- at δ1.2-1.45 (bs, 18H), Ala C^{α}H-C$\underline{H}_3$ at δ1.3 (s, 3H), C^{α}-$\underline{H}$ of (Cys, Tyr, His, Trp, Thr, Pro, Ser, & Ala) amino acids at δ3.4-4.9 (m, 12H), Ser C^{β}-$\underline{H}_2$ at δ 3.2-4.12 (m, 2H), Pro C^{β}-$\underline{H}_2$ at δ 2.0-2.2 (m, 2H), Pro C^{γ}-$\underline{H}_2$ at δ 1.9-2.1 (m, 2H), Pro C^{δ}-$\underline{H}_2$ at δ 3.3-3.5 (m, 2H), Thr –CH-C$\underline{H}$(CH_3)-OH at δ 4.6 (m, 1H), Thr –CH-CH(C$\underline{H}_3$)-OH at δ 1.2 (m, 3H), Tyr C^{β}-$\underline{H}_2$ at δ 3.2-3.45 (m, 2H), Tyr –CH_2-$C_6\underline{H}_4$-OH at δ 6.5-6.9 (m, 4H), Trp C^{β}-$\underline{H}_2$ at δ 3.0-3.4 (m, 2H), Trp –CH_2-$C_8\underline{H}_5$NH at δ 7.1-8.3 (m, 5H), His C^{β}-$\underline{H}_2$ at δ 2.9-3.15 (m, 2H), His –CH_2-$C_3\underline{H}_2N_2$H at δ 8.2-8.7 (m, 2H), Cys C^{β}-$\underline{H}_2$ at δ 2.9-3.2 (m, 2H) (**Fig. S3**).

Fluorescence cadaverine (FC) and dodecanol (DC) were conjugated to the carboxyl groups of mPEG-PCC by EDC/HOBT coupling reaction. At the end of reaction, FC conjugated copolymer was purified using isopropanol and diethyl ether and by extensive dialysis and lyophilized. ^{1}H NMR (500 MHz, DMSO-d_6) spectra of mPEG-b-PCC-g-FC-g-DC showed peaks corresponding to PEG (−C$\underline{H}_2$−C$\underline{H}_2$−O) at δ3.5, PCC (−CO-O-C$\underline{H}_2$- & CH_3-C(CO)-C$\underline{H}_2$) at δ4.2 (m, 4H), C$\underline{H}_3$-$(CH_2)_9$- at δ0.9 (t, 3H), CH_3-(C$\underline{H}_2$)$_9$- at δ1.2-1.45 (bs, 18H), -CO-NH-CH_2-(C$\underline{H}_2$)$_3$- at δ1.2-1.6 (m, 6H), -CS-NH-C$\underline{H}_2$- & -CO-NH-C$\underline{H}_2$- at δ2.6-3.2 (m, 4H), -CS-N$\underline{H}$-CH_2- & -CO-N$\underline{H}$-CH_2- at δ (m, 2H), -NH-$C_6\underline{H}_3(CO_2H)$-$C_{13}\underline{H}_6O_2$(OH) at δ6.1-7.9 (m, 9H) (**Fig. S4**).

GEM and DC were conjugated to the carboxyl groups of mPEG-PCC to get GEM-conjugated copolymers. ^{1}H NMR spectra of mPEG-PCC showed peaks corresponding to PEG (−CH_2−CH_2−O) at δ3.5 and PCC (−CH_2−) at δ4.2. Absence of benzene protons at δ7.3 confirmed complete hydrogenation along with the presence of -

COOH peaks at δ12-14 as reported earlier.[17] Based on the peak integrals of mPEG and PCC protons, an average molecular weight of mPEG-PCC was calculated to be ~9600 Da with 29 PCC units. GEM and DC were conjugated onto the carboxyl groups of mPEG-PCC by EDC/HOBT coupling reaction and GEM conjugated copolymer was purified by precipitation in isopropanol and diethyl ether followed by extensive dialysis and lyophilization. ^{1}H NMR (500 MHz, DMSO-d_6) of mPEG-b-PCC-g-GEM-g-DC showed peaks corresponding to PEG (−C$\underline{H}_2$−C$\underline{H}_2$−O) at δ3.5, PCC (−CO-O-C$\underline{H}_2$- & CH_3-C(CO)-C$\underline{H}_2$) at δ4.2 (m, 4H), C$\underline{H}_3$-$(CH_2)_9$- at δ0.9 (t, 3H), CH_3-(C$\underline{H}_2)_9$- at δ1.2-1.45 (bs, 18H), GEM 5'- and 3'–OH groups at δ6.18-6.39 (m, 2H), -CO-N$\underline{H}$- at δ8.26 (m, 1H), -CO-N-C$\underline{H}$=CH- at δ8.15 (m, 1H) and -CO-N-CH=C$\underline{H}$- at δ5.35 (m, 1H) (**Fig. S5**).

3.2. Formulation development and characterization

Mixed micellar formulations have been successfully applied for drug delivery application.[32, 33] Various block copolymers at a certain molar or weight ratios are used for mixed micelles formation and they formed single polymeric micellar system rather than two separate micelles.[34, 35] In our previous report, we synthesized mPEG-b-PCC-g-GEM-g-DC copolymer for GEM delivery by passive targeting only. In the present study, we have conjugated GE11 peptide to our polymeric micelles for EGFR receptor mediated active targeting. However, GE11 peptide, GEM and DC conjugation in the same micellar system created synthetic complexity and reduced drug loading (data not shown). To avoid these obstacles, we synthesized GE11-PEG-PCD and mPEG-b-PCC-g-GEM-g-DC copolymers separately and prepared EGFR targeted mixed micelles by combining GE11-PEG-PCD (10-30% weight ratio) and mPEG-b-PCC-g-GEM-g-DC (70-90% weight ratio) copolymers by film hydration. In addition, we used HW12-PEG-

PCD/mPEG-b-PCC-g-GEM-g-DC (30/70 w/w) mixed micelles. mPEG-b-PCC-g-GEM-g-DC had a mean particle size of 26 ± 3 nm with a PDI of 0.27. We measured particle size and surface ζ- potential of GE11-linked mixed micelles (10-30% weight ratios) and HW12-linked (30/70 w/w ratio) mixed micelles to determine effect of GE11 or HW12 conjugation on size and surface charge of mixed micelles. Unmodified micelles had a mean particle size of 26 ± 3 nm (PDI-0.27), whereas GE11-linked mixed micelles (10-30% weight ratio) and HW12-linked mixed micelles (30% weight ratio) had a mean particle size of 51 ± 5 (PDI-0.229), and 53 ± 0.8 (PDI-0.188), respectively indicating the conjugation of GE11 or HW12 peptide did not significant change the size of mixed micelles than mPEG-b-PCC-g-GEM-g-DC micelles. We observed increased in surface ζ–potential of GE11-linked mixed micelles (10-30% weight ratio) -6.8 ± 2 mV and HW12-linked mixed micelles (30% weight ratio) -5.9± 0.2 mV as compared to unmodified micelles -4.6 ± 0.2 mV. GEM loading in mPEG-b-PCC-g-GEM-g-DC was calculated by ^{1}H NMR, which showed GEM 5'-and 3'–OH protons at δ 5.90 and δ 6.2 respectively. The presence of amide proton at δ8.26 confirmed the formation of amine bond with pendant carboxyl group of mPEG-PCC, which is in agreement with the literatures.[7, 36, 37] GEM loading in mPEG-b-PCC-g-GEM-g-DC was ~14.8% w/w by integrating and calculating amide protons peak at δ8.26 (**Fig. S5**). However ^{1}H-NMR analysis can only confirm the chemical conjugation of GEM to the polymer backbone but cannot predict accurate drug loading. Therefore, GEM loading in mPEG-b-PCC-g-GEM-g-DC was further determined by alkaline hydrolysis and then analyzed by HPLC-UV method as reported previously.[17] GEM loading in micelles was found ~12% w/w (data not shown). Although, our mPEG-b-PCC-g-GEM-g-DC copolymer (12% w/w drug

loading) showed higher drug loading than previously reported PEGylated GEM derivatives (0.98-6.79% w/w drug loading range), but it was lower than reported GEM−squalene nanoassemblies (GEM loading of 41% w/w).[7, 8, 38-40] PEGylated gemcitabine nanoassemblies were achieved by addition of PEG−squalene or PEG−cholesterol (1:0.7 w/w) which showed decrease in gemcitabine loading but higher efficacy than gemcitabine−squalene nanoassemblies. Therefore, our formulation is a balanced between PEG coating (55%) and GEM loading (12 % w/w). Though our formulation needs improvement to increase GEM payload but this polymeric drug conjugate offers numerous advantages over the squalenoylated nanoassemblies. Gemcitabine−squalene nanoassemblies are rapidly cleared from the bloodstream by the reticulo-endothelial system (RES) due to absence of PEG coating.[16] PEG coating in outer shell needed for stealth effect and to reduce opsonization and blood clearance. Our micelles had a much smaller particle size (25-50 nm) than gemcitabine−squalene nanoassemblies (140 nm) and presence of PEG (~55%) coating in our formulation can provide stealth effect. In our previous study, we found a controlled release pattern of GEM (39% GEM release in 10 days) from the micelles even in the presence of proteolytic enzyme Cathepsin B.[17] Based on that we assume that all our formulations had similar drug release patterns.

3.3. EGFR-mediated uptake of GEM conjugated GE11-modified mixed micelles

To convert mixed micellar system into cell surface probe as well as to verify receptor mediated GEM delivery in vitro and in vivo, we conjugated FC as fluorescent tag to carboxyl terminated mPEG-PCC copolymer via amide bond. Various fluorescein molecules are widely used to label nanoparticles for intracellular and intra-tumoral

distribution of nanoparticles.[41, 42] We selected FC as a fluorescein substance since prior reports showed that carboxylic acids of proteins, water soluble biopolymer and difluorinated cyclooctyne (DIFO) chemically conjugated with the primary aliphatic amine of FC through EDAC coupling for subcellular distribution, interaction between cell surface receptor and ligand, and in vivo imaging.[43, 44] Therefore, we synthesized FC conjugated mPEG-b-PCC-g-FC-g-DC copolymer. We prepared FC labeled GE11-linked mixed micelles (10-30% weight ratios) and unmodified micelles. Before cellular uptake of labeled mixed micelles in MIA PaCa-2 cells, we determined EGFR expression levels in MIA PaCa-2 cells by flow cytometry. MIA PaCa-2 cells showed high expression of EGFR (**Fig. S6**). To determine whether GE11 peptide enhanced the cellular uptake by EGFR expressing MIA PaCa-2 cells, cells were incubated with FC labeled GE11-linked mixed micelles and unmodified micelles for 12 h. The fluorescein images are shown in **Fig. S7** for qualitative analysis of cellular uptake. MIA PaCa-2 cells treated with GE11-linked mixed micelles at 30% w/w ratios showed significantly higher fluorescence than GE11-linked mixed micelles at 10 and 20% weight ratios and unmodified micelles (**Fig. S7 A, B, C&D**). To confirm, GE11 and not HW12 is an EGFR ligand, we also prepared FC labeled HW12-linked mixed micelles at 30% weight ratio and cells were incubated with FC labeled GE11-linked mixed micelles and HW12-linked mixed micelles at 30% weight ratio for 12 h respectively. The fluorescein images of MIA PaCa-2 cells treated with GE11-linked mixed micelles at 30% weight ratio showed stronger fluorescence compared to HW12-linked mixed micelles, suggesting that mixed micelles containing GE11 peptide could facilitate cellular delivery of conjugated drugs (**Fig. S7E).** To further confirm the ligand receptor interaction and specific role of GE11 peptide, we pre-

saturated MIA PaCa-2 cells with free GE11 peptide prior to incubation with GE11-linked mixed micelles at 30% weight ratio. Results depicted in (**Fig. S7 F**) showed significant reduction of the fluorescence signal and comparable fluorescence signal of HW12-linked mixed micelles treated cells (**Fig. S7 E**), supporting EGFR receptor mediated uptake. Cellular uptake results were further analyzed by flow cytometry for quantitative analysis. Results delineated in **Fig. 3 A, B, C & D** clearly indicated that the mean

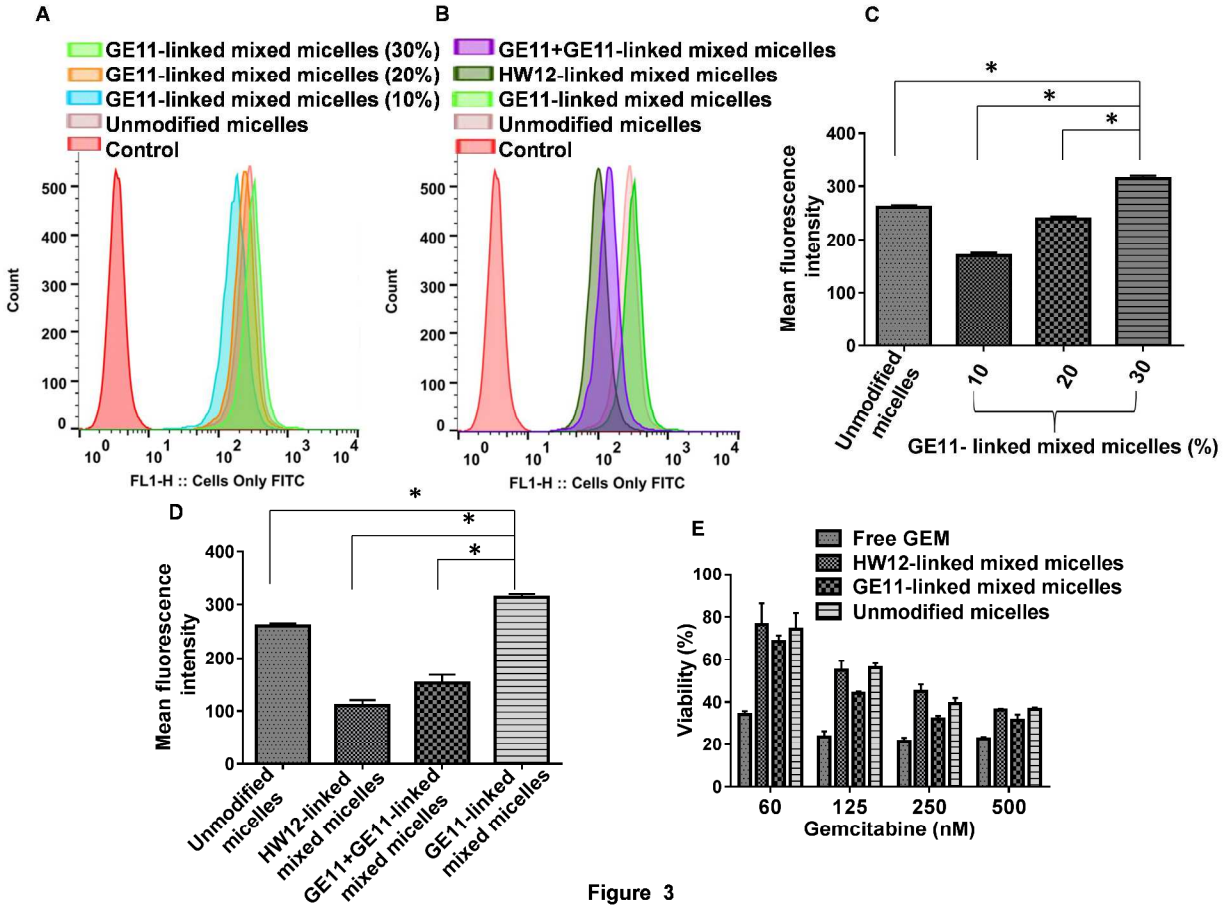

Figure 3

fluorescence intensity of GE11-linked mixed micelles (30% w/w) treated cells were 1.2 fold and 3.1 fold higher than unmodified micelles and HW12-linked mixed micelles respectively. However, we observed the cellular uptake of HW12-linked mixed micelles was lower than unmodified micelles. The exact mechanism for this lower uptake of peptide linked mixed micelles require additional investigation, but it may be due to the

increase in hydrophillicity of HW12 peptide. To illustrate this point, we calculated hydrophobicity for GE11 (YHWYGYTPQNVI) peptide which was 50 whereas for HW12 (HYPYAHPTHPSW) 33.33 suggesting, HW12-linked micelles more hydrophilic as compared to GE11-linked mixed micelles. This increase in hydrophilicity is expected to decrease cellular uptake as shown in **Fig 3.** [45] When pre-treated cells with free GE11 peptide prior incubation of cells with GE11-linked mixed micelles (30% w/w) mixed micelles, the mean fluorescence intensity decreased significantly (**Fig. 3 B & D**).

3.4. In vitro cytotoxicity studies

Density of surface ligand is critical to target cell binding in vitro as well as pharmacokinetic profiles in vivo. Our cellular uptake study clearly indicated that 30% w/w ratios of GE11-linked mixed micelles was superior to HW12-linked mixed micelles and unmodified micelles. Therefore, we prepared GE11-linked mixed micelles (GE11-PEG-PCD/mPEG-b-PCC-g-GEM-g-DC) at 30% w/w ratios to enhance receptor mediated cellular uptake. Similarly, we prepared HW12-linked mixed micelles using HW12-PEG-PCD and mPEG-b-PCC-g-GEM-g-DC copolymers at 30% weight ratio. For cytotoxicity studies, MIA PaCa-2 cells were treated with GE11-linked mixed micelles, HW12-linked mixed micelles, unmodified micelles and free GEM. Free GEM exhibited highest cytotoxicity within the studied concentration range compared to GE11-linked mixed micelles, HW12-linked mixed micelles, unmodified micelles, indicated by lowering cell viability (**Fig. 3E**). Although free GEM showed maximum toxicity but its plasma instability and lack of target specificity would restrict its in vivo tumor inhibition capability. GE11-linked mixed micelles showed a higher cytotoxicity than HW12-linked mixed micelles and unmodified micelles at all GEM concentrations tested, further

demonstrating that GE11 peptide play important role for anti-tumor efficacy in GE11 modified mixed micelles (**Fig. 3E**). The IC_{50} value was calculated for GE11-linked mixed micelles (95.32 nM), which was 1.2 fold and 1.3 fold lower than unmodified micelles (116.91 nM) and HW12-linked mixed micelles (126.58 nM) respectively. Our results are in good agreement with the literature. For example, Chen et al. demonstrated that a GE11 density of 10% is enough to enable EGFR-ligand binding.[25] In their study, the cell viability for liposomes with a 15% GE11 density was similar to that for liposomes with a 10% GE11 density.

3.5. GE11 peptide conjugated mixed micelles for targeting EGFR expressing pancreatic tumor as well as tumor neovasculature

After in vitro efficacy of GE11-linked mixed micelles, we determined targeting efficiency of GE11-linked mixed micelles in orthotopic pancreatic tumor bearing athymic nude mice by systemic administration of FC labeled GE11-linked mixed micelles, HW12-linked mixed micelles and unmodified micelles. FC labeled GE11-linked mixed micelles injected mouse tumor sections showed higher fluorescence intensity at 24 h post injection than FC labeled HW12-linked mixed micelles and unmodified micelles injected tumor sections (**Fig. 4**), supporting that GE11 peptide facilitated distribution and accumulation of drug molecule into the tumor. Our results are in good agreement with the work of Xu et al. who demonstrated enhanced accumulation of GE11 peptide conjugated gelatin nanoparticles in subcutaneous Panc-1 pancreatic tumor model especially at early time points.[26] Previous reports showed that tumor cells as well as tumor derived endothelial cells express EGFR.[46] Toward confirming GE11-linked mixed micelles can target tumor as well as tumor neovaculature under in vivo condition, we

stained same tumor sections with rabbit polyclonal anti-VE-cadherin antibody (markers of tumor endothelial cells) and counterstained with Alexa Fluor 594 F(ab')2 fragment of

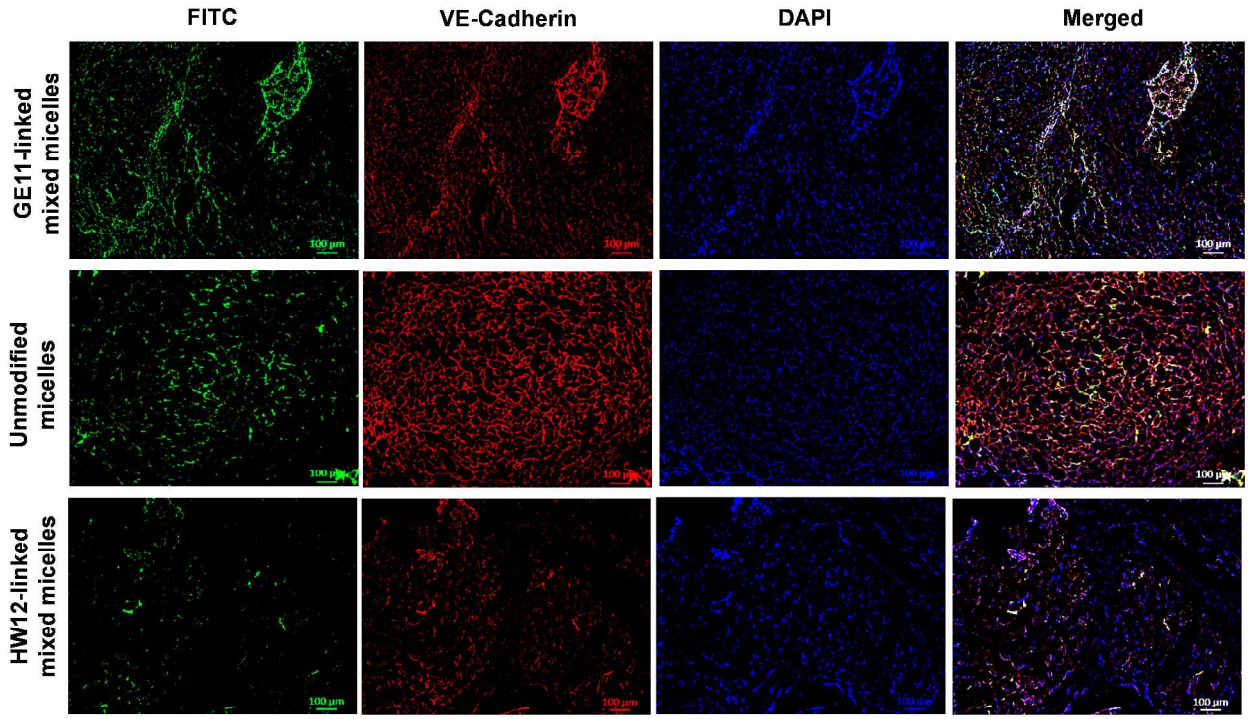

Figure 4

goat anti-rabbit IgG (H+L) secondary antibody. When tumor sections were observed under a fluorescent microscope, the merged image of FC labeled GE11-linked mixed micelles mouse tumor sections showed that targeted mixed micelles deliver FC dye to tumor as well as tumor vasculature. In contrast, FC labeled HW12-linked mixed micelles and unmodified micelles did not deliver FC dye to tumor vasculature. Therefore, our result demonstrated in **Fig. 4A** clearly indicated that GE11-linked mixed micelles not only capable of delivering drug to tumor cells but also effective in distributing drug to tumor vasculature.

3.6. In vivo efficacy in orthotopic pancreatic tumor model

After demonstrating the ability of GE11-linked mixed micelles to target EGFR expressing tumor as well as tumor endothelial cells, we investigated whether GE11-linked mixed micelles could inhibit orthotopic pancreatic tumor growth. After orthotopically implanting MIA PaCa-2/luciferase tumor cells in the pancreas, mice were intravenously administered GE11-linked mixed micelles, HW12-linked mixed micelles, unmodified micelles and free GEM at an equivalent dose of 40 mg/kg GEM three times in a week after 12 days of cell implantation. We selected this dose according to our previous report and this dose is lower than the maximum tolerated dose (MTD) of GEM.[17] In vivo efficacy of GEM in mice numerous reports showed wide range of its dose ranging from 7mg/kg to 500 mg/kg for intraperitoneal route and intravenous route of administration.[40, 47-49] At day 12, all mice in different group were noninvasively imaged for luciferase bioluminescence to determine the tumor growth and randomized for treatment. Tumor growth inhibitions of different formulations were monitored by measuring luciferase bioluminescence at different time points during the treatment (day 12, 16, 20, 24, 26 and 30) and photon counts was calculated by Living Image® 3.2 software (Caliper Life Science). Final bioluminescence images were taken at day 30 and images depicted in **Fig. 5A** clearly showed significant tumor growth inhibition in mice treated with GE11-linked mixed micelles compared to HW12-linked mixed micelles, unmodified micelles and free GEM. We compared photon counts between different groups after plotting photon value versus days after treatment (**Fig. 5B**). This result further strengthened our in vitro observation and signified GE11 important role for EGFR targeting. HW12 decorated HW12-linked mixed micelles showed minimal tumor growth effect, supporting that GE11 peptide is EGFR targeting ligand not HW12

peptide. Unmodified micelles showed better tumor growth inhibition than free GEM. We

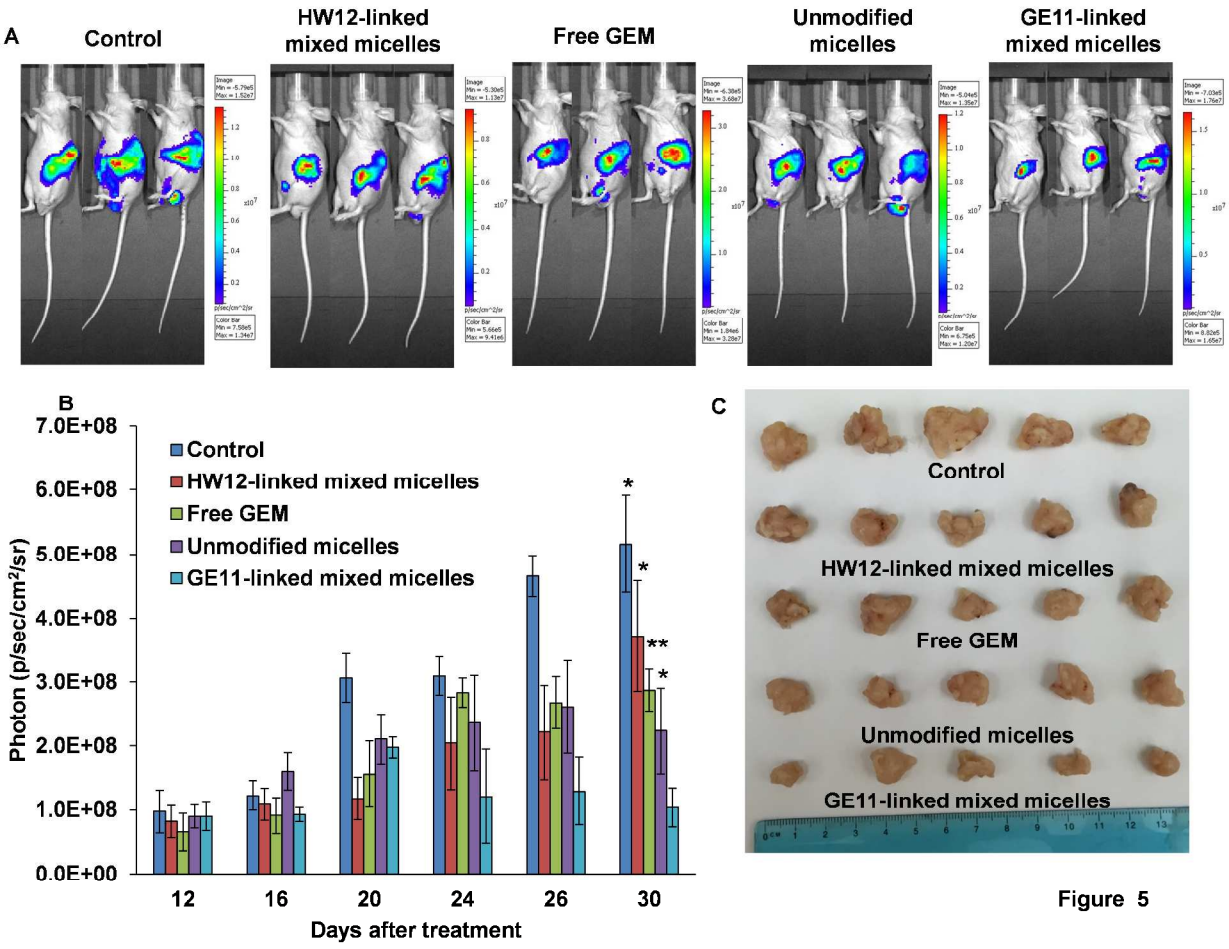

Figure 5

removed all tumors from different group, measured tumor volume and weight and taken images of tumor after sacrificing the mice at the end of the experiment. Tumor images as shown in **Fig. 5C** confirmed remarkable tumor growth inhibition capability of GE11-linked mixed micelles compared to HW12-linked mixed micelles, unmodified micelles and free GEM. This was further confirmed by measuring the tumor volume and weight (**Fig. 6 A&B**). Mouse body weight was taken during the treatment course to monitor the

adverse effect of GEM. **Fig. 6C** clearly indicated that our in vivo GEM dose (40 mg/kg) did not show any abnormal body weight change in all the experimental groups.

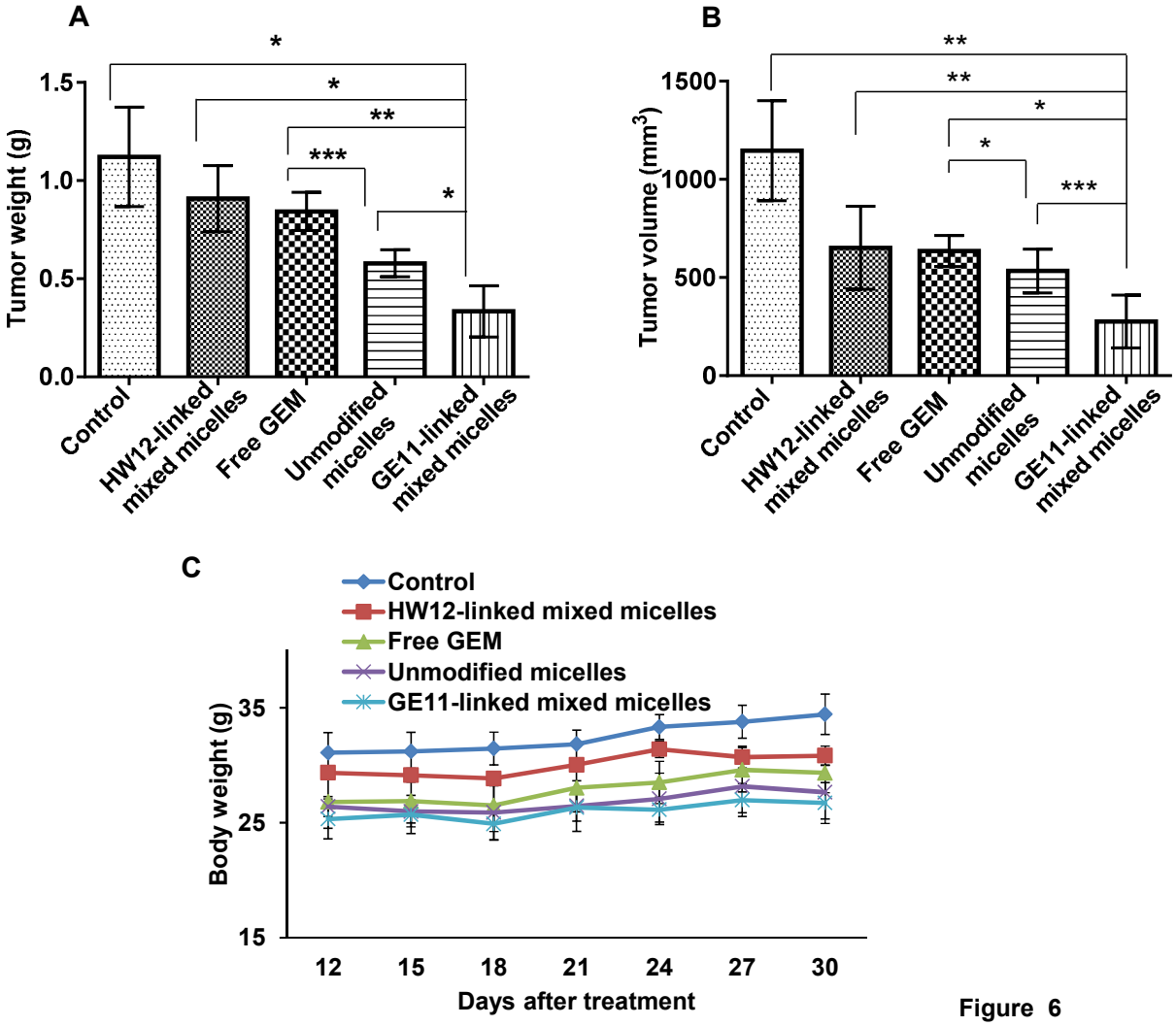

Figure 6

Immunohistochemical analysis was done for Ki-67, cleaved caspase-3 and H&E staining of tumor cryosections obtained from all treated groups. Unmodified micelles treated mice showed reduction in Ki-67 staining and increase in cleaved caspase-3 staining compared to the free GEM.

Mice treated with GE11-linked mixed micelles showed least Ki-67 staining and highest cleaved caspase-3 staining (**Fig. 7A&B**). GE11-linked mixed micelles and

unmodified micelles treated groups showed more necrotic areas compared to HW12-linked mixed micelles, free GEM and control (**Fig. 7C**). GE11-linked mixed micelles treatment showed more necrotic areas compared to unmodified micelles, supporting the beneficial effect of GE11 peptide mediated active targeting over passive targeting. After three doses of treatment, major organs, such as heart, liver and kidney were collected from all treated groups. Histological staining of these organs did not show any

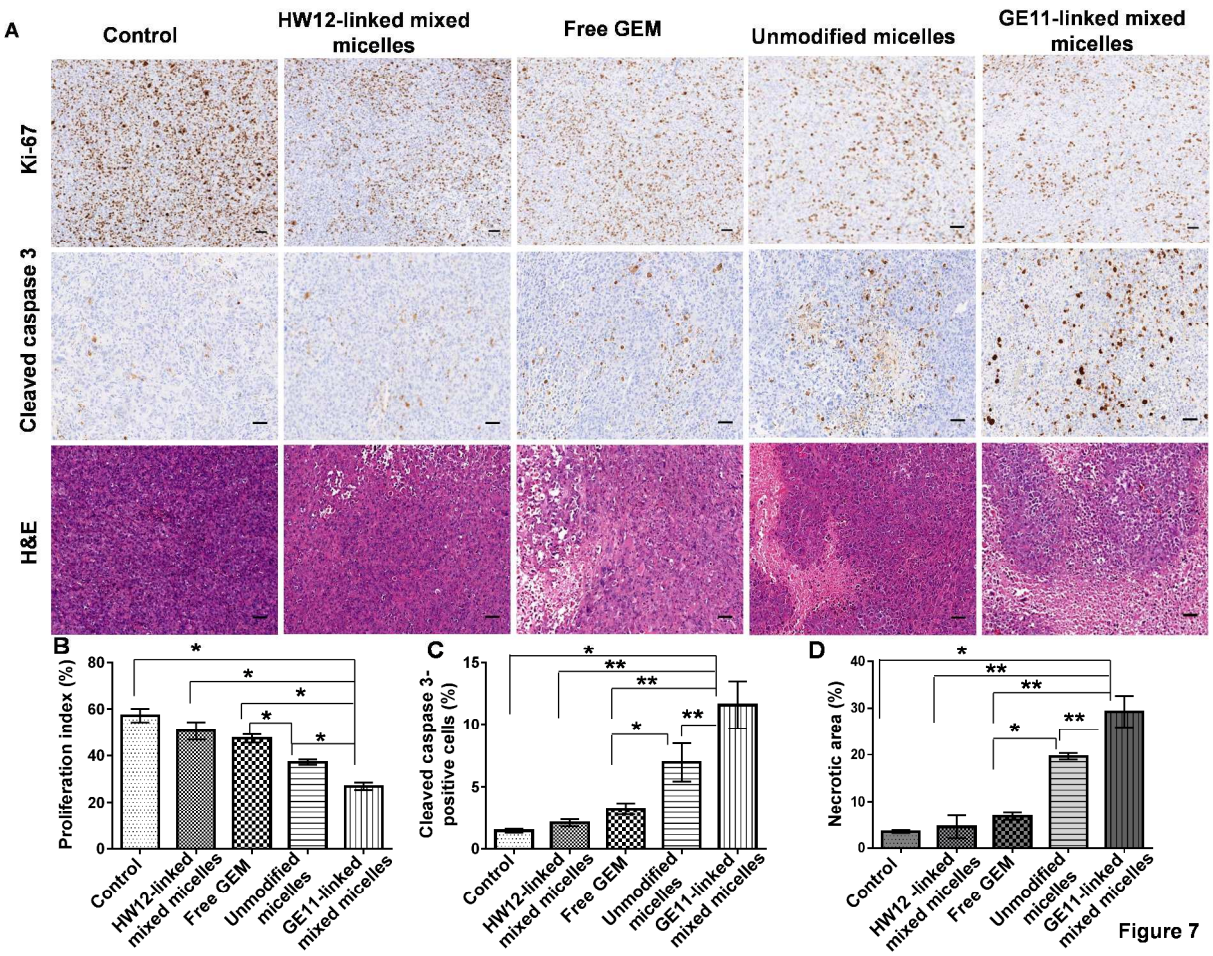

Figure 7

pathological changes after treatment in all the groups (**Fig. S8**). Tumor growth inhibition

potential of GE11-linked mixed micelles and unmodified micelles were confirmed by TUNEL assay. Mice treated with GE11-linked mixed micelles showed enhanced apoptosis of cancer cells compared to control, free GEM, HW12-linked mixed micelles and unmodified micelles treated mice (**Fig. 8**). Solid tumors growth and metastatic potential to distant organs critically depend on angiogenesis, sprouting of new blood

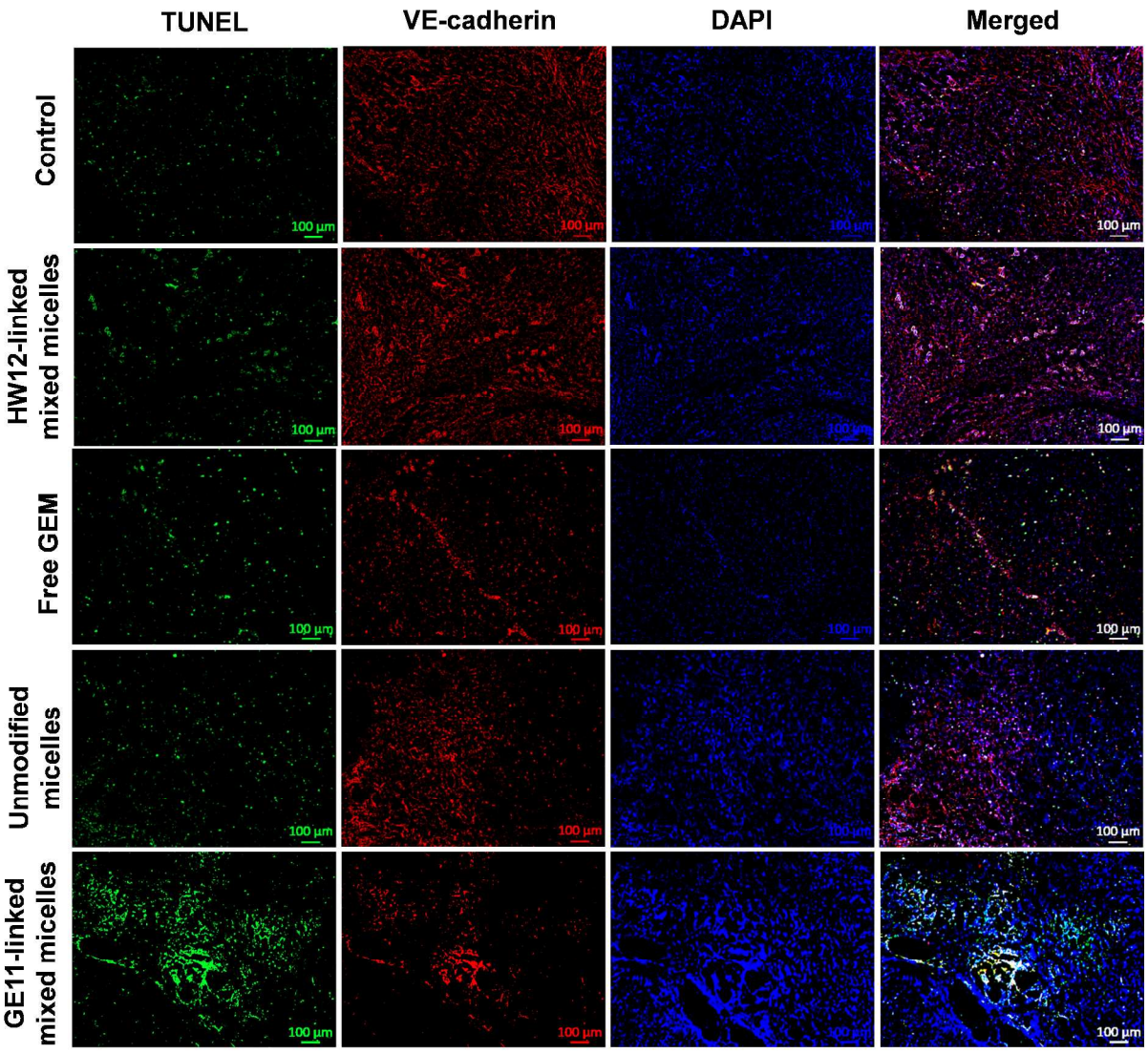

Figure 8

vessels from pre-existing blood vessels.[19] The newly formed blood vessels are structurally and functionally abnormal than normal blood vessels. Delivery of anti-

angiogenic agent specifically to tumor derived endothelial cells is an attractive strategy for anti-angiogenic cancer therapy. GEM shows its anti-cancer activity by mainly cytotoxic action on cancer cells.[50] In addition to its cytotoxic action, recent study showed that it also has anti-angiogenic activity.[51, 52] Previous in vitro studies showed that GEM is more sensitive to endothelial cells than pancreatic cancer cells.[51] GEM is hydrophilic drug and its plasma instability hinders its delivery into tumor endothelial cells in vivo.

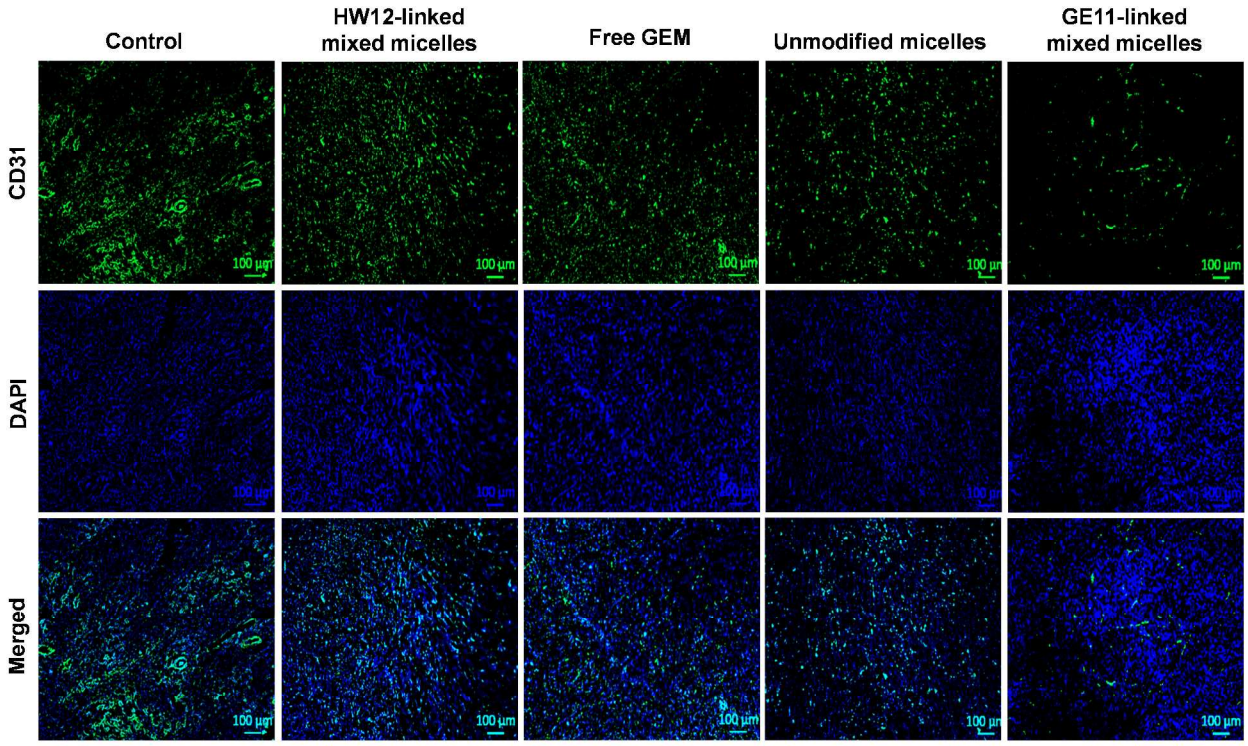

Figure 9

We previously described that conjugation of GEM to polymer increased its in vivo stability. Further, we showed in our model drug distribution study using FC conjugated polymeric system that GE11-linked mixed micelles deliver FC dye in tumor derived endothelial cells. We co-immunostained the same TUNEL stained tumor sections with rabbit polyclonal anti-VE-cadherin (marker of endothelial cells) to determine the apoptosis of tumor endothelial cells. Result delineated in **Fig. 8** showed mice treated

with GE11-linked mixed micelles induced significant apoptosis of tumor endothelial cells, supporting significant tumor growth inhibition potential of this mixed micellar system.

In animal model, inhibition of the angiogenesis can efficiently reduce pancreatic tumor growth.[47, 53-55] Further, vascular abnormality leads to complex tumor environment with impaired blood flow and interstitial hypertension, which hinders delivery of anti-cancer drugs and oxygen.[56] The reduction of this abnormal vasculature improves delivery of chemotherapy to tumor tissues.[57] CD31 is a 130 kDa transmembrane glycoprotein, one of the best markers of benign and malignant tumor vessels.[58] Tumor cryosections were immunostained with CD31 antibody to determine the anti-vascular efficacy of GE11-linked mixed micelles. Our immunohistological staining data showed significantly reduced tumor microvessel density in GE11-linked mixed micelles group compared to control, free GEM, HW12-linked mixed micelles and unmodified micelles treated groups (**Fig. 9**). TUNEL assay and microvessel density results clearly showed that GE11-linked mixed micelles ta rget cancer cells as well as tumor vasculature. All these results demonstrate that the significant inhibition potential of GEM conjugated GE11-modified mixed micelles in a orthotopic pancreatic tumor mouse model.

4. CONCLUSIONS

In summary, we have developed an EGFR targeted GEM conjugated polymeric mixed micelles for treating pancreatic cancer. GE11-linked mixed micelles specifically and efficiently delivered GEM to EGFR expressing pancreatic cancer, interacted with tumor blood vessels and showed significant inhibition of pancreatic tumor growth in

orthotopic mouse model. Thus, GE11-linked mixed micelles is a promising carrier for drug delivery to treat various EGFR expressing cancers.

SUPPORTING INFORMATION

The Supporting Information is available free of charge via the internet at http://pubs.acs.org

^{1}H-NMR of spectra of co-polymers, EGFR expression in MIA PaCa-2 cells, Epifluorescence microscopic images of cells treated with co-polymers, hematoxylin and eosin (H&E) staining of major organs (liver, heart and kidney).

ACKNOWLEDGMENTS

This work was supported by the National Institutes of Health (1R01EB017853), Fred and Pamela Buffet Cancer Center and the Faculty Start-up fund to RIM.

FIGURE LEGENDS

Figure 1. Synthesis scheme of GE11-PEG-PCD (A), Chemical structure of HW12-PEG-PCD (B). Reagents : (i) KOH, DMF, benzyl bromide, 100°C, 15 h; (ii) triphosgene, pyridine, CH_2Cl_2, -78 to 0°C; (iii) 10% Pd/C, H_2, ethyl acetate, RT, 40 psi, 3 h; (iv) EDC, HOBT, TEA, DMF, dodecanol, RT, 18 h; (v) DBU, CH_2Cl_2, MAL-PEG_{5000}-OH, RT, 3 h.; (vi) MAL-PEG-PCD, DMSO: distilled water (1:1 v/v), GE11 peptide (CYHWYGYTPQNVI), TECP (100 mM), RT, N_2, 24 h.

Figure 2. Synthesis scheme of mPEG-PCC-g-FC-g-DC (A) Chemical structure of mPEG-PCC-g-GEM-g-DC (B). Reagents : (i) KOH, DMF, benzyl bromide, 100°C, 15 h; (ii) triphosgene, pyridine, CH_2Cl_2, -78 to 0°C; (iii) DBU, CH_2Cl_2, methoxy-PEG5000-OH, RT, 3 h; (iv) 10% Pd/C, H_2, ethyl acetate, RT, 40 psi, 3 h; (v) EDC, HOBT, DIPEA, DMF, dodecanol, fluorescein cadaverine (FC), RT, 48 h.

Figure 3. Flow cytometry analysis of cellular uptake of fluorescein cadaverine (FC) labeled micelles showing histogram and the mean fluorescence intensity of MIA PaCa-2 cells treated with GE11-linked mixed micelles (10-30% w/w), unmodified micelles (mPEG-b-PCC-g-FC-g-DC) (A&C), *$p<0.001$; GE11-linked mixed micelles (30% w/w), pre-incubation of MIA PaCa-2 cells with free GE11 prior incubation of cells with GE11-linked mixed micelles (30/70 w/w), unmodified micelles and HW12-linked mixed micelles (30/70 w/w)

(B&D). Effect of GEM on MIA PaCa-2 cell viability (E) *p<0.001 compared to GE11-linked mixed micelles.

Figure 4. In vivo tumor as well as tumor vasculature targeting of labeled micellar system. Male athymic nude mice were orthotopically implanted with MIA PaCa-2 tumor. Fluorescein cadaverine (FC) labelled GE11-linked mixed micelles; unmodified micelles and HW12-linked mixed micelles were intravenously administered at day 21. After 24 h, the mice were sacrificed; tumors were removed, for sectioning and immunostaining with anti-VE-cadherin (marker of endothelial cells). GE11-linked mixed micelles significantly accumulated in tumor neovasculature whereas unmodified micelles and HW12-linked mixed micelles poorly accumulated in the tumor neovasculature. Scale bar, 100 μm.

Figure 5. In vivo efficacy of GE11-linked mixed micelles after systemic administration in orthotopic pancreatic tumor bearing mice. A representative bioluminescence image from the mice treated with a saline, free GEM, HW12-linked mixed micelles, unmodified micelles and GE11-linked mixed micelles (n=5) (A). Relative photon intensity plot of all groups were measured from day 12 to day 30 (B). Data represented as the mean ± SEM. *p<0.05; **p<0.001 compared to GE11-linked mixed micelles. Representative tumor sizes of each group were taken after sacrificing the mice at the end of the experiment (C).

Figure 6. Tumor volume (A) and tumor weight (B) were measured after sacrificing the mice at the end of the experiment. For all graphs, each data point represents the mean ± SEM. (n = 5) *p<0.001, **p<.0001, ***p<0.05 (A) and *p<0.001, **p<0.05, ***p<0.005. Body weight of all groups were measured from day 12 to day 30 (C).

Figure 7. Immunohistochemical analysis of tumor samples for Ki-67 (cell proliferation marker), cleaved caspase 3 (apoptosis marker) and hematoxylin and eosin (H&E) staining (A). Saline, free GEM, HW12-linked mixed micelles, unmodified micelles and GE11-linked mixed micelles treated tumor samples were cryosectioned, fixed and immunostained for Ki-67, cleaved caspase 3 and H&E (A). Statistical analysis was performed for Ki-67 (B), *p<0.001; cleaved caspase 3 (C), *p<0.05; **p<0.01 and H&E (C), *p<0.01; **p<0.001. Scale bar, 2 mm.

Figure 8. Detection of apoptosis induced by GE11-linked mixed micelles in tumor and tumor endothelial cells of the orthotopic pancreatic tumor. Saline, HW12-linked mixed micelles, Free GEM, unmodified micelles and GE11-linked mixed micelles treated tumor samples were cryosectioned, fixed and immunostained for TUNEL-positive nuclei (green), VE-cadherin (endothelial cells, red) and DAPI (blue) stained nuclei (red). Scale bar, 100 μm.

Figure 9. Immunostaining of cryosections for CD31 as marker for microvessel density. GE11-linked mixed micelles treated tumor section showed significant reduction of microvessel densities. Saline, HW12-linked mixed micelles, Free

GEM, unmodified micelles and GE11-linked mixed micelles treated tumor samples were cryosectioned, fixed and immunostained with rat anti-mouse CD31 antibody (green) and DAPI-stained nuclei (blue). Scale bar, 100 μM.

REFRENCES

1. Ko, A. H.; Truong, T. G.; Kantoff, E.; Jones, K. A.; Dito, E.; Ong, A.; Tempero, M. A. *Cancer Chemother. Pharmacol.* **2012***, 70*, 875-881.

2. Wang, Z.; Sengupta, R.; Banerjee, S.; Li, Y.; Zhang, Y.; Rahman, K. M.; Aboukameel, A.; Mohammad, R.; Majumdar, A. P.; Abbruzzese, J. L.; Sarkar, F. H. *Cancer Res.* **2006***, 66*, 7653-7660.

3. Kumar, V.; Mondal, G.; Slavik, P.; Rachagani, S.; Batra, S. K.; Mahato, R. I. *Mol. Pharm.* **2015***, 12*, 1289-1298.

4. Oberstein, P. E.; Saif, M. W. *JOP* **2011***, 12*, 96-100.

5. Plunkett, W.; Huang, P.; Xu, Y. Z.; Heinemann, V.; Grunewald, R.; Gandhi, V. *Semin. Oncol.* **1995***, 22*, 3-10.

6. Burris, H. A.,3rd; Moore, M. J.; Andersen, J.; Green, M. R.; Rothenberg, M. L.; Modiano, M. R.; Cripps, M. C.; Portenoy, R. K.; Storniolo, A. M.; Tarassoff, P.; Nelson, R.; Dorr, F. A.; Stephens, C. D.; Von Hoff, D. D. *J. Clin. Oncol.* **1997***, 15*, 2403-2413.

7. Pasut, G.; Canal, F.; Dalla Via, L.; Arpicco, S.; Veronese, F. M.; Schiavon, O. *J. Control. Release* **2008***, 127*, 239-248.

8. Vandana, M.; Sahoo, S. K. *Biomaterials* **2010***, 31*, 9340-9356.

9. Bornmann, C.; Graeser, R.; Esser, N.; Ziroli, V.; Jantscheff, P.; Keck, T.; Unger, C.; Hopt, U. T.; Adam, U.; Schaechtele, C.; Massing, U.; von Dobschuetz, E. *Cancer Chemother. Pharmacol.* **2008***, 61*, 395-405.

10. Cosco, D.; Bulotta, A.; Ventura, M.; Celia, C.; Calimeri, T.; Perri, G.; Paolino, D.; Costa, N.; Neri, P.; Tagliaferri, P.; Tassone, P.; Fresta, M. *Cancer Chemother. Pharmacol.* **2009***, 64*, 1009-1020.

11. Maksimenko, A.; Mougin, J.; Mura, S.; Sliwinski, E.; Lepeltier, E.; Bourgaux, C.; Lepetre, S.; Zouhiri, F.; Desmaele, D.; Couvreur, P. *Cancer Lett.* **2013***, 334*, 346-353.

12. Celia, C.; Malara, N.; Terracciano, R.; Cosco, D.; Paolino, D.; Fresta, M.; Savino, R. *Nanomedicine* **2008***, 4*, 155-166.

13. Moog, R.; Burger, A. M.; Brandl, M.; Schuler, J.; Schubert, R.; Unger, C.; Fiebig, H. H.; Massing, U. *Cancer Chemother. Pharmacol.* **2002***, 49*, 356-366.

14. Fan, M.; Liang, X.; Li, Z.; Wang, H.; Yang, D.; Shi, B. *Eur. J. Pharm. Sci.* **2015***, 79*, 20-26.

15. Tao, X. M.; Wang, J. C.; Wang, J. B.; Feng, Q.; Gao, S. Y.; Zhang, L. R.; Zhang, Q. *Eur. J. Pharm. Biopharm.* **2012***, 82*, 401-409.

16. Reddy, L. H.; Khoury, H.; Paci, A.; Deroussent, A.; Ferreira, H.; Dubernet, C.; Decleves, X.; Besnard, M.; Chacun, H.; Lepetre-Mouelhi, S.; Desmaele, D.; Rousseau, B.; Laugier, C.; Cintrat, J. C.; Vassal, G.; Couvreur, P. *Drug Metab. Dispos.* **2008***, 36*, 1570-1577.

17. Chitkara, D.; Mittal, A.; Behrman, S. W.; Kumar, N.; Mahato, R. I. *Bioconjug. Chem.* **2013***, 24*, 1161-1173.

18. Kunjachan, S.; Pola, R.; Gremse, F.; Theek, B.; Ehling, J.; Moeckel, D.; Hermanns-Sachweh, B.; Pechar, M.; Ulbrich, K.; Hennink, W. E.; Storm, G.; Lederle, W.; Kiessling, F.; Lammers, T. *Nano Lett.* **2014***, 14*, 972-981.

19. Carmeliet, P.; Jain, R. K. *Nature* **2000***, 407*, 249-257.

20. Yu, D. H.; Lu, Q.; Xie, J.; Fang, C.; Chen, H. Z. *Biomaterials* **2010***, 31*, 2278-2292.

21. Valetti, S.; Maione, F.; Mura, S.; Stella, B.; Desmaele, D.; Noiray, M.; Vergnaud, J.; Vauthier, C.; Cattel, L.; Giraudo, E.; Couvreur, P. *J. Control. Release* **2014***, 192*, 29-39.

22. Chitkara, D.; Singh, S.; Kumar, V.; Danquah, M.; Behrman, S. W.; Kumar, N.; Mahato, R. I. *Mol. Pharm.* **2012***, 9*, 2350-2357.

23. Patra, C. R.; Bhattacharya, R.; Wang, E.; Katarya, A.; Lau, J. S.; Dutta, S.; Muders, M.; Wang, S.; Buhrow, S. A.; Safgren, S. L.; Yaszemski, M. J.; Reid, J. M.; Ames, M. M.; Mukherjee, P.; Mukhopadhyay, D. *Cancer Res.* **2008***, 68*, 1970-1978.

24. Li, Z.; Zhao, R.; Wu, X.; Sun, Y.; Yao, M.; Li, J.; Xu, Y.; Gu, J. *FASEB J.* **2005***, 19*, 1978-1985.

25. Cheng, L.; Huang, F. Z.; Cheng, L. F.; Zhu, Y. Q.; Hu, Q.; Li, L.; Wei, L.; Chen, D. W. *Int. J. Nanomedicine* **2014***, 9*, 921-935.

26. Xu, J.; Gattacceca, F.; Amiji, M. *Mol. Pharm.* **2013***, 10*, 2031-2044.

27. Tang, H.; Chen, X.; Rui, M.; Sun, W.; Chen, J.; Peng, J.; Xu, Y. *Mol. Pharm.* **2014***, 11*, 3242-3250.

28. Li, F.; Danquah, M.; Mahato, R. I. *Biomacromolecules* **2010***, 11*, 2610-2620.

29. Wang, H. X.; Xiong, M. H.; Wang, Y. C.; Zhu, J.; Wang, J. *J. Control. Release* **2013***, 166*, 106-114.

30. Zhang, W.; Shi, Y.; Chen, Y.; Ye, J.; Sha, X.; Fang, X. *Biomaterials* **2011***, 32*, 2894-2906.

31. Danquah, M.; Fujiwara, T.; Mahato, R. I. *Biomaterials* **2010***, 31*, 2358-2370.

32. Mu, C. F.; Balakrishnan, P.; Cui, F. D.; Yin, Y. M.; Lee, Y. B.; Choi, H. G.; Yong, C. S.; Chung, S. J.; Shim, C. K.; Kim, D. D. *Biomaterials* **2010***, 31*, 2371-2379.

33. O'Neil, C. P.; van der Vlies, A. J.; Velluto, D.; Wandrey, C.; Demurtas, D.; Dubochet, J.; Hubbell, J. A. *J. Control. Release* **2009***, 137*, 146-151.

34. Yin, H.; Lee, E. S.; Kim, D.; Lee, K. H.; Oh, K. T.; Bae, Y. H. *J. Control. Release* **2008***, 126*, 130-138.

35. Bae, Y.; Diezi, T. A.; Zhao, A.; Kwon, G. S. *J. Control. Release* **2007***, 122*, 324-330.

36. Cavallaro, G.; Licciardi, M.; Salmaso, S.; Caliceti, P.; Gaetano, G. *Int. J. Pharm.* **2006***, 307*, 258-269.

37. Khare, V.; Kour, S.; Alam, N.; Dubey, R. D.; Saneja, A.; Koul, M.; Gupta, A. P.; Singh, D.; Singh, S. K.; Saxena, A. K.; Gupta, P. N. *Int. J. Pharm.* **2014**, *470*, 51-62.

38. Reddy, L. H.; Dubernet, C.; Mouelhi, S. L.; Marque, P. E.; Desmaele, D.; Couvreur, P. *J. Control. Release* **2007**, *124*, 20-27.

39. Rejiba, S.; Reddy, L. H.; Bigand, C.; Parmentier, C.; Couvreur, P.; Hajri, A. *Nanomedicine* **2011**, *7*, 841-849.

40. Reddy, L. H.; Renoir, J. M.; Marsaud, V.; Lepetre-Mouelhi, S.; Desmaele, D.; Couvreur, P. *Mol. Pharm.* **2009**, *6*, 1526-1535.

41. Weissleder, R.; Nahrendorf, M.; Pittet, M. J. *Nat. Mater.* **2014**, *13*, 125-138.

42. Trehin, R.; Figueiredo, J. L.; Pittet, M. J.; Weissleder, R.; Josephson, L.; Mahmood, U. *Neoplasia* **2006**, *8*, 302-311.

43. Gordon, E. J.; Gestwicki, J. E.; Strong, L. E.; Kiessling, L. L. *Chem. Biol.* **2000**, *7*, 9-16.

44. Baskin, J. M.; Prescher, J. A.; Laughlin, S. T.; Agard, N. J.; Chang, P. V.; Miller, I. A.; Lo, A.; Codelli, J. A.; Bertozzi, C. R. *Proc. Natl. Acad. Sci. U. S. A.* **2007**, *104*, 16793-16797.

45. Peetla, C.; Rao, K. S.; Labhasetwar, V. *Mol. Pharm.* **2009**, *6*, 1311-1320.

46. Amin, D. N.; Hida, K.; Bielenberg, D. R.; Klagsbrun, M. *Cancer Res.* **2006**, *66*, 2173-2180.

47. Bruns, C. J.; Shrader, M.; Harbison, M. T.; Portera, C.; Solorzano, C. C.; Jauch, K. W.; Hicklin, D. J.; Radinsky, R.; Ellis, L. M. *Int. J. Cancer* **2002***, 102*, 101-108.

48. Sun, F. X.; Tohgo, A.; Bouvet, M.; Yagi, S.; Nassirpour, R.; Moossa, A. R.; Hoffman, R. M. *Cancer Res.* **2003***, 63*, 80-85.

49. Bruns, C. J.; Harbison, M. T.; Davis, D. W.; Portera, C. A.; Tsan, R.; McConkey, D. J.; Evans, D. B.; Abbruzzese, J. L.; Hicklin, D. J.; Radinsky, R. *Clin. Cancer Res.* **2000***, 6*, 1936-1948.

50. Storniolo, A. M.; Allerheiligen, S. R.; Pearce, H. L. *Semin. Oncol.* **1997***, 24*, S7-2-S7-7.

51. Laquente, B.; Lacasa, C.; Ginesta, M. M.; Casanovas, O.; Figueras, A.; Galan, M.; Ribas, I. G.; Germa, J. R.; Capella, G.; Vinals, F. *Mol. Cancer. Ther.* **2008***, 7*, 638-647.

52. Amoh, Y.; Li, L.; Tsuji, K.; Moossa, A. R.; Katsuoka, K.; Hoffman, R. M.; Bouvet, M. *J. Surg. Res.* **2006***, 132*, 164-169.

53. Khan, A. W.; Dhillon, A. P.; Hutchins, R.; Abraham, A.; Shah, S. R.; Snooks, S.; Davidson, B. R. *Eur. J. Surg. Oncol.* **2002***, 28*, 637-644.

54. Jia, L.; Zhang, M. H.; Yuan, S. Z.; Huang, W. G. *World J. Gastroenterol.* **2005***, 11*, 447-450.

55. Zhang, X.; Galardi, E.; Duquette, M.; Lawler, J.; Parangi, S. *Clin. Cancer Res.* **2005***, 11*, 5622-5630.

56. Padera, T. P.; Stoll, B. R.; Tooredman, J. B.; Capen, D.; di Tomaso, E.; Jain, R. K. *Nature* **2004***, 427*, 695.

57. Jain, R. K. *Nat. Med.* **2001***, 7*, 987-989.

58. Pusztaszeri, M. P.; Seelentag, W.; Bosman, F. T. *J. Histochem. Cytochem.* **2006***, 54*, 385-395.

TABLE OF CONTENTS GRAPHIC